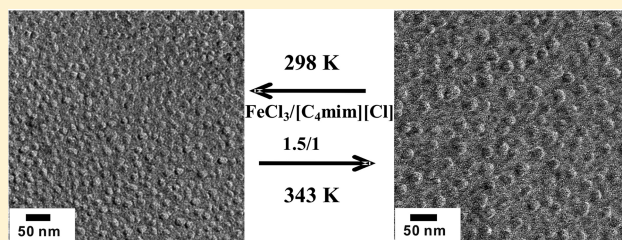


Ionic Structures of Nanobased $\text{FeCl}_3/[\text{C}_4\text{mim}]\text{Cl}$ Ionic LiquidsJi-Guang Li,[†] Yu-Feng Hu,^{*,†} Shu-Feng Sun,[‡] Shan Ling,[†] and Jin-Zhu Zhang[†][†]State Key Laboratory of Heavy Oil Processing and High Pressure Fluid Phase Behavior & Property Research Laboratory, China University of Petroleum, Beijing 102249, China[‡]The Centre for Biological Imaging, Institute of Biophysics, Chinese Academy of Sciences, Beijing 100101, China

ABSTRACT: We synthesized a series of $\text{FeCl}_3/[\text{C}_4\text{mim}]\text{Cl}$ (iron(III) chloride with 1-butyl-3-methylimidazolium chloride) ionic liquids. The temperature dependence of the Raman spectra of the $\text{FeCl}_3/[\text{C}_4\text{mim}]\text{Cl}$ ionic liquids was measured for the first time to analyze their ionic species. In addition, the infrared spectra, thermodynamic properties, and freeze-fracture transmission electron microscopy were combined together with the Raman spectra to reveal the microscopic information of the $\text{FeCl}_3/[\text{C}_4\text{mim}]\text{Cl}$ ionic liquids. When the mole ratio of $\text{FeCl}_3/[\text{C}_4\text{mim}]\text{Cl}$ is less than 1, the Raman scattering identifies the presence of $[\text{FeCl}_4]^-$ in the ionic liquid. When FeCl_3 is in excess, $[\text{Fe}_2\text{Cl}_7]^-$ begins to appear. Besides, we found that the relative intensity of the two symmetry vibrations of $[\text{Fe}_2\text{Cl}_7]^-$ is changing as the temperature is varied. The strength of the interionic interactions in $\text{FeCl}_3/[\text{C}_4\text{mim}]\text{Cl}$ ionic liquids follows the order $1/1.5 > 1.5/1 > 1/1$ due to the formation of $[\text{FeCl}_4]^-$ and $[\text{Fe}_2\text{Cl}_7]^-$. The nanostructures in $\text{FeCl}_3/[\text{C}_4\text{mim}]\text{Cl}$ ionic liquids were observed for the first time by using biological imaging. The sizes of the local domains are found to be tens of nanometers.



1. INTRODUCTION

Ionic liquids are composed solely of ions and are liquid at ambient temperature.^{1–3} For their specific properties, such as nonflammability, high thermal stability, wide temperature range in the liquid state and extremely low volatility, they are attracting more and more interest as alternatives to conventional molecular liquids.^{1–3}

$\text{FeCl}_3/[\text{C}_4\text{mim}]\text{Cl}$ ionic liquids have all characteristics of conventional ionic liquids including high temperature stability, high solvation ability, general nonflammability, wide liquidus range, and negligible vapor pressure.^{4–9} Compared to conventional ionic liquids, magnetic $\text{FeCl}_3/[\text{C}_4\text{mim}]\text{Cl}$ ionic liquids have some unique characteristics: strong magnetic field response,^{4–9} paramagnetic,^{4,10} possible local ordering of the magnetic anions,^{8,10} single-component materials that are free from phase separation,⁴ and moisture-stable and intermediate Lewis acidity.^{11,12} It is even expected that ferromagnetic ionic liquids will be synthesized in the near future.⁸ Magnetic ionic liquids $\text{FeCl}_3/[\text{C}_4\text{mim}]\text{Cl}$ were discovered as a key material for green chemistry on solvents and catalysts in these years.^{5,13,14} Recently, nanostructured conducting polymers were synthesized by simply adding monomers into a 1/1 $\text{FeCl}_3/[\text{C}_4\text{mim}]\text{Cl}$ ionic liquid, and magnetic field seems to affect these local structures and hence the resultant polymer nanostructures.^{6,9,15} These facts suggest that magnetic ionic liquids could be widely used as magnetic liquids consisting of nanoparticles.⁴ When $\text{FeCl}_3/[\text{C}_4\text{mim}]\text{Cl}$ ionic liquids are involved in green process, we can find that ionic species, interionic interactions, and temperature dependence of nanostructures are key factors.^{5,6,9,13–15} However, the microscopic information about the ionic state remains incompletely understood and there are no available reports regarding the nanostructure of $\text{FeCl}_3/$

$[\text{C}_4\text{mim}]\text{Cl}$ ionic liquids. Therefore, it is of great importance to understand the temperature-dependence of the structures of the $\text{FeCl}_3/[\text{C}_4\text{mim}]\text{Cl}$ ionic liquids.

In this work, the temperature-dependence of the Raman spectra of $\text{FeCl}_3/[\text{C}_4\text{mim}]\text{Cl}$ ionic liquids was measured for the first time. In addition, the infrared (IR) spectra, conductivity, and glass transition results were combined to compare to the Raman spectra results and to investigate the interionic interactions between ions. The temperature dependence of liquid nanostructures of $\text{FeCl}_3/[\text{C}_4\text{mim}]\text{Cl}$ ionic liquids was measured for the first time using freeze-fracture transmission electron microscopy (FF-TEM).

2. EXPERIMENTAL DETAILS

2.1. Materials. Anhydrous FeCl_3 with the purity of more than 98% was purchased from Acros and used without further purification. *N*-methylimidazole and *n*- $\text{C}_4\text{H}_9\text{Cl}$ with the claimed purities of >99% were supplied by Shanghai Jiachen Chemical Co., Ltd., and were refined by the traditional methods before use. $\text{FeCl}_3/[\text{C}_4\text{mim}]\text{Cl}$ ionic liquids were prepared using the well-established procedures of our and other previous works.^{5,8,16} Both the literature results⁵ and our preliminary experiments showed that, after having been dried in a vacuum box at 333 K for 24 h, the prepared ionic liquids could be dried to constant weights. Therefore, the ionic liquids were dried in the vacuum box at 333 K for 24 h and then were dried in the vacuum box at 333 K for another one or two 24 h to make sure the ionic liquids were of constant weight. Finally, the ionic

Received: July 17, 2011

Revised: December 22, 2011

Published: December 28, 2011

liquids were further dried using 3 Å molecular sieves for 3 days immediately prior to use.

2.2. Methods. In order to observe the effect of temperature on the changeability of the nanodomains and of the Raman bands of the $\text{FeCl}_3/[\text{C}_4\text{mim}]\text{Cl}$ ionic liquids and to compare the FF-TEM and the Raman spectra results in a mild condition, the present FF-TEM images and Raman spectra were measured at 298 and 343 K.

For the FF-TEM measurements, the samples were injected into the sample holders (gold stub of sample carriers for knife fracture). For temperature tests, the holders with samples were placed into an oven at the desired temperature. More than half an hour was allowed to achieve thermal equilibrium. Then, samples in the holders were immersed rapidly into liquid ethane cooled in advance with liquid nitrogen. Subsequently, they were rapidly transferred into liquid nitrogen. The samples put into the chamber of the freeze-etching apparatus (BALZERS BAF-400D) were fractured at 150 K at a pressure of 3×10^{-7} mbar. After being etched for 1 min at 163 K, Pt–C was sprayed onto the fracture face at 45° until it reached 20 nm thickness, and then, C was sprayed at 90° with 150 nm thickness. Coated samples (in replicate) were removed from the chamber, were dipped first into dimethyl benzene, then washed with ethanol and finally with double-distilled water. The replicate samples were mounted onto grids and viewed with a transmission electron microscope (PHILIPS-FEI TECNAI20).

The Raman spectra were obtained using a HR800 micro-Raman spectrometer (Jobin Yvon, France) employing a 785 nm laser beam, with an instrument resolution of 0.5 cm^{-1} . Sample temperatures ranging from 298 to 343 K were controlled using a Linkam TS600 hot stage with a temperature stability of $\pm 0.5 \text{ K}$. The previous study¹⁷ using this spectrometer showed that 5 min is long enough to achieve the thermalization of the system; therefore, in this study, the temperature was held fixed for at least 5 min at each selected temperature (298 and 343 K) in order to obtain the thermalization of the system. The Raman spectra were measured in both crossed $Z(XY)\bar{Z}(VH)$ and parallel $Z(XY)\bar{Z}(VV)$ polarizations, where X, Y, and Z are the cubic axes. The temperature was measured with a PT100 with an evaluating standard uncertainty of $\pm 0.006 \text{ K}$.

The glass transition temperatures were measured using a differential scanning calorimeter (DSC),¹⁶ model TA Q2000, with a heating rate of 10 K min^{-1} , and the temperature was calibrated by indium. The IR spectra were taken on KBr pellets with a Nicolet Magna-IR 560 spectrophotometer ($400\text{--}4000 \text{ cm}^{-1}$).¹⁰

3. RESULTS AND DISCUSSION

Figure 1 shows the Raman spectra of the ionic liquids, respectively, containing the $\text{FeCl}_3/[\text{C}_4\text{mim}]\text{Cl}$ ratio of 1/1.5 and 1/1 at 298 and 343 K. The strong features at ~ 333 and $\sim 384 \text{ cm}^{-1}$ belonging to $[\text{FeCl}_4]^-$ in the examined ionic liquids correspond very well with the literature values.^{5,18} Note that Wang et al.⁵ have reported the ESI-MS (electrospray ionization-mass spectrum) of the 1/1 $\text{FeCl}_3/[\text{C}_4\text{mim}]\text{Cl}$ ionic liquid at room temperature. Their result also identified the presence of $[\text{FeCl}_4]^-$ in this ionic liquid. Those results mean that, after strong exothermic reaction between FeCl_3 and $[\text{C}_4\text{mim}]\text{Cl}$, the $[\text{FeCl}_4]^-$ anion is the main iron(III)-containing species in the ionic liquids where the ratio of $\text{FeCl}_3/[\text{C}_4\text{mim}]\text{Cl}$ is less than or equal to 1/1.

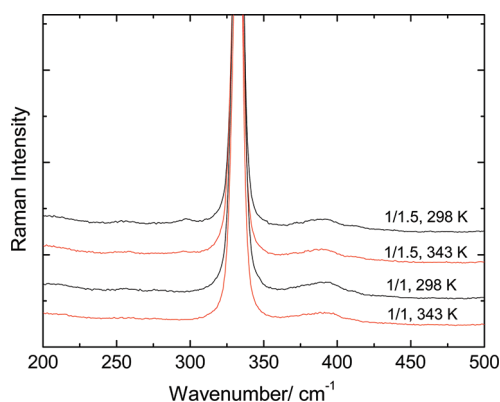


Figure 1. Temperature dependence of Raman spectra of 1/1.5 and 1/1 $\text{FeCl}_3/[\text{C}_4\text{mim}]\text{Cl}$ ionic liquids at 298 and 343 K.

As can be seen in Figure 2, except for the peak at 333 cm^{-1} due to $[\text{FeCl}_4]^-$, the features at ~ 260 and $\sim 420 \text{ cm}^{-1}$ belong to

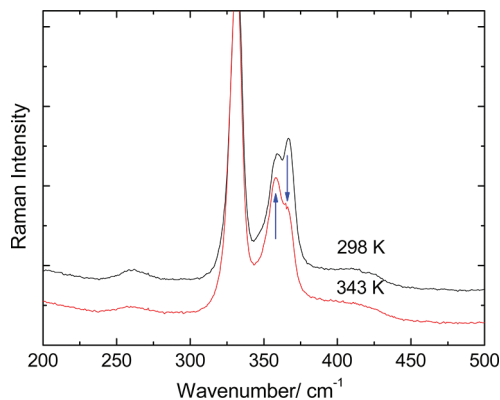


Figure 2. Temperature dependence of the Raman spectra of 1.5/1 $\text{FeCl}_3/[\text{C}_4\text{mim}]\text{Cl}$ ionic liquid at 298 and 343 K.

$[\text{Fe}_2\text{Cl}_7]^-$ when FeCl_3 is in excess.^{18,19} Compared to Raman spectra of 1/1.5 and 1/1 $\text{FeCl}_3/[\text{C}_4\text{mim}]\text{Cl}$ ionic liquids, the 360 and $\sim 367 \text{ cm}^{-1}$ bands are new strong features for the 1.5/1 $\text{FeCl}_3/[\text{C}_4\text{mim}]\text{Cl}$ ionic liquid. According to the prediction of unrestricted Hartree–Fock calculations,¹⁸ the 360 and $\sim 367 \text{ cm}^{-1}$ features should be assigned to two symmetry vibrations of the C_2 structure of $[\text{Fe}_2\text{Cl}_7]^-$. In addition, the ESI-MS of the 1.5/1 $\text{FeCl}_3/[\text{C}_4\text{mim}]\text{Cl}$ ionic liquid at room temperature also indicated the existence of $[\text{Fe}_2\text{Cl}_7]^-$ in this ionic liquid.²⁰ This conclusion is also supported by the fact that a Raman peak has been reported at 360 cm^{-1} in high-temperature FeCl_3 molten salts and has been assigned to $[\text{Fe}_2\text{Cl}_7]^-$ in these systems.²¹ These results provide a strong evidence for the formation of $[\text{Fe}_2\text{Cl}_7]^-$ in the $(1.5 \text{ FeCl}_3)/(1 [\text{C}_4\text{mim}]\text{Cl})$ ionic liquid. On the basis of these Raman spectra results, the IR spectra were combined to offer distinctive information about interionic interactions in $\text{FeCl}_3/[\text{C}_4\text{mim}]\text{Cl}$ ionic liquids.^{22,23}

Figure 3 shows the IR spectra of the (1/1.5, 1/1, and 1.5/1) $\text{FeCl}_3/[\text{C}_4\text{mim}]\text{Cl}$ ionic liquids at room temperature. The characteristic frequency bands at $\sim 3149 \text{ cm}^{-1}$ of 1/1 and 1.5/1 $\text{FeCl}_3/[\text{C}_4\text{mim}]\text{Cl}$ ionic liquids and at $\sim 3147 \text{ cm}^{-1}$ of 1/1.5 $\text{FeCl}_3/[\text{C}_4\text{mim}]\text{Cl}$ ionic liquid are assigned to the stretching modes of C(4)–H or C(5)–H bond of the imidazolium ring.^{10,24} The downshift of 1/1.5 $\text{FeCl}_3/[\text{C}_4\text{mim}]\text{Cl}$ ionic liquid by ca. 2 cm^{-1} might be due to the stronger interionic interactions in 1/1.5 $\text{FeCl}_3/[\text{C}_4\text{mim}]\text{Cl}$ in comparison with

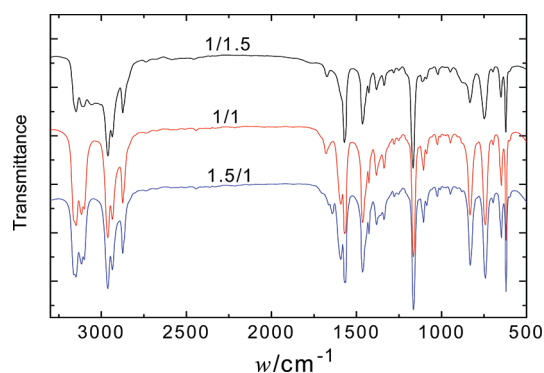


Figure 3. IR spectra of $\text{FeCl}_3/[\text{C}_4\text{mim}]\text{Cl}$ ionic liquids at room temperature.

those in 1/1 and 1.5/1 $\text{FeCl}_3/[\text{C}_4\text{mim}]\text{Cl}$ arising from better delocalization of charge on the atoms of the Cl^- than that of $[\text{FeCl}_4]^-$ and $[\text{Fe}_2\text{Cl}_7]^-$. The characteristic frequency bands at $\sim 833\text{ cm}^{-1}$ of 1/1 $\text{FeCl}_3/[\text{C}_4\text{mim}]\text{Cl}$ and at $\sim 831\text{ cm}^{-1}$ of 1.5/1 $\text{FeCl}_3/[\text{C}_4\text{mim}]\text{Cl}$ belong to aliphatic C–H vibrations.²⁴ The downshift of 1.5/1 $\text{FeCl}_3/[\text{C}_4\text{mim}]\text{Cl}$ by ca. 2 cm^{-1} might be attributed to the stronger interionic interactions in 1.5/1 $\text{FeCl}_3/[\text{C}_4\text{mim}]\text{Cl}$ in comparison with those in 1/1 $\text{FeCl}_3/[\text{C}_4\text{mim}]\text{Cl}$ arising from greater polarizability of $[\text{Fe}_2\text{Cl}_7]^-$ than that of $[\text{FeCl}_4]^-$. It can be concluded from these IR results that the interionic interactions in $\text{FeCl}_3/[\text{C}_4\text{mim}]\text{Cl}$ ionic liquids obey the order $1/1.5 > 1.5/1 > 1/1$. These results can be further established from conductivity and glass forming behaviors.

As shown in Figure 4, recently, we have shown that the conductivity increases extremely when the mole ratio of $\text{FeCl}_3/$

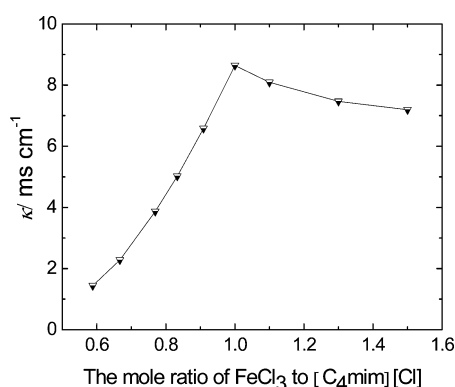


Figure 4. Mole ratio of $\text{FeCl}_3/[\text{C}_4\text{mim}]\text{Cl}$ dependence of conductivities of $\text{FeCl}_3/[\text{C}_4\text{mim}]\text{Cl}$ ionic liquids at 298 K.²⁵

$[\text{C}_4\text{mim}]\text{Cl}$ is less than 1/1 and decreases smoothly when the mole ratio of $\text{FeCl}_3/[\text{C}_4\text{mim}]\text{Cl}$ is greater than 1/1.²⁵ The extreme increase in conductivity can be due to the rapidly decreased interionic interactions, while the smooth decrease in conductivity can be attributed to the slowly increased interionic interactions.

Figure 5 shows a clear evidence for the presence of glass transitions in those ionic liquids where the ratio of $\text{FeCl}_3/[\text{C}_4\text{mim}]\text{Cl}$ is 1/1.5, 1/1, or 1.5/1 upon increasing temperature. The glass transition temperature (T_g) increases from 1/1 ($T_g = 185\text{ K}$) through 1.5/1 ($T_g = 189\text{ K}$) to 1/1.5 ($T_g = 204\text{ K}$). This trend is consistent with the order for the interionic interactions that was revealed by the present IR results and the

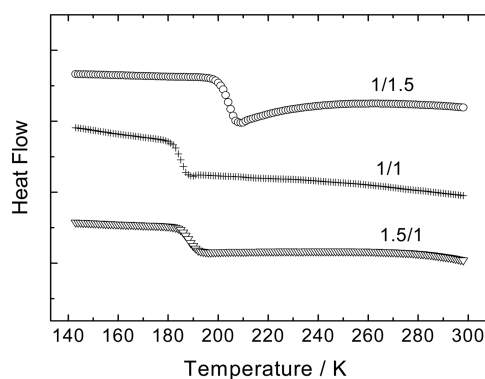
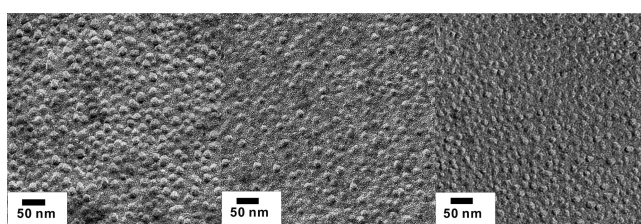
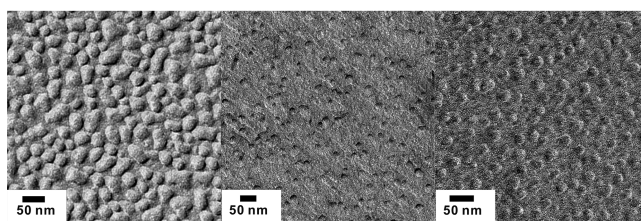


Figure 5. Differential scanning calorimetry (DSC) traces of the 1/1.5, 1/1, and 1.5/1 $\text{FeCl}_3/[\text{C}_4\text{mim}]\text{Cl}$ ionic liquids on heating.

literature results.¹⁰ Of course, the apparently greater T_g of the 1/1.5 $\text{FeCl}_3/[\text{C}_4\text{mim}]\text{Cl}$ ionic liquid relative to those of the 1/1 and 1.5/1 $\text{FeCl}_3/[\text{C}_4\text{mim}]\text{Cl}$ ionic liquids may be attributed to the fact that the nanodomains formed in the examined ionic liquids at the lower temperature are apparently more extensive in the former ionic liquid than in the latter two ionic liquids (see Figure 6).



(1/1.5, 1/1, and 1.5/1) $\text{FeCl}_3/[\text{C}_4\text{mim}]\text{Cl}$ at 298 K



(1/1.5, 1/1, and 1.5/1) $\text{FeCl}_3/[\text{C}_4\text{mim}]\text{Cl}$ at 343 K

Figure 6. FF-TEM images of the nanostructures formed in $\text{FeCl}_3/[\text{C}_4\text{mim}]\text{Cl}$.

The FF-TEM images of 1/1.5, 1/1, and 1.5/1 $\text{FeCl}_3/[\text{C}_4\text{mim}]\text{Cl}$ ionic liquids were shown in Figure 6. The nanostructures can be formed in the $\text{FeCl}_3/[\text{C}_4\text{mim}]\text{Cl}$ ionic liquids. The molecular simulation results have shown that the cation chains of ionic liquids could aggregate to form spatially heterogeneous domains.²⁶ In addition, ESI-MS has been used to investigate the ionic aggregates in particular in halo-metalate ionic liquids.^{27,28}

The sizes of the local domains of the $\text{FeCl}_3/[\text{C}_4\text{mim}]\text{Cl}$ ionic liquids are several tens of nanometers. These agree well with the sizes of the nanodomains of $[\text{C}_n\text{mim}][\text{PF}_6]$ ($n = 4, 6, 8$) that were established by coherent anti-Stokes Raman scattering.²⁹ The nanodomains of $\text{FeCl}_3/[\text{C}_4\text{mim}]\text{Cl}$ ionic liquids are apparently softening as the temperature increases from 298 to 343 K, implying that the nanodomains tend to melt at higher temperatures. It is clear from Figures 1 and 2 that the variation of the relative intensities of the Raman bands

of the 1.5/1 FeCl₃/[C₄mim]Cl ionic liquid with temperature is larger than that of 1/1.5 and 1/1 FeCl₃/[C₄mim]Cl ionic liquids. At the same time, the variation of the nanostructures with the temperature increases in the order 1/1.5 < 1/1 ≈ 1.5/1. These comparisons reveal that the thermal variability of the nanostructures strongly correlates with the thermal changeability of the anion. The present results also show that the compactness of the nanostructures at 298 K increases in the order 1.5/1 ≈ 1/1 < 1/1.5. Combined use of these results reveals that the dependence of ionic species on the mole ratio of FeCl₃/[C₄mim]Cl plays a significant role on the formation of nanostructures in FeCl₃/[C₄mim]Cl ionic liquids.

4. CONCLUSIONS

In summary, the temperature-dependence of the Raman spectra of FeCl₃/[C₄mim]Cl ionic liquids was measured to analyze the ionic structure. The results were used together with the IR, conductivity, and glass transition results to investigate the interionic interactions between ions. When the mole ratio of FeCl₃/[C₄mim]Cl is less than 1/1, Raman scattering indicates the presence of FeCl₄[−]. When FeCl₃ is in excess, [Fe₂Cl₇][−] begins to appear, and the relative intensity of its two symmetry vibrations is changing with increasing temperature. The interionic interactions in FeCl₃/[C₄mim]Cl ionic liquids follow the order 1/1.5 > 1.5/1 > 1/1 due to the formation of [FeCl₄][−] and [Fe₂Cl₇][−]. The temperature dependence of the nanostructures of FeCl₃/[C₄mim]Cl ionic liquids were revealed for the first time using FF-TEM, and the sizes of local domains are tens of nanometers. The present results show that the compactness of the nanostructures increases in the order 1.5/1 ≈ 1/1 < 1/1.5. The present findings reveal the ionic structure and nanodomains of FeCl₃/[C₄mim]Cl ionic liquids, and open up a new avenue to design FeCl₃/[C₄mim]Cl ionic liquids with tunable chemistry and morphology. The present results are important for us to optimize gas absorption or separations, to tune catalytic selectivity, and to prepare the desired anisotropic, zeolitic, and polymer materials. These findings can also give us a new angle of view to understand the nature of ionic liquids.

AUTHOR INFORMATION

Corresponding Author

*E-mail: huyf3581@sina.com.

ACKNOWLEDGMENTS

We thank the National Natural Science Foundation of China (20976189, 21076224, 20925623, and 21036008) and Science Foundation of China University of Petroleum, Beijing (qzdx-2011-01) for financial support.

REFERENCES

- (1) Dupont, J.; de Souza, R. F.; Suarez, P. A. Z. *Chem. Rev.* **2002**, *102*, 3667–3692.
- (2) Song, C. E. *Chem. Commun.* **2004**, 1033–1043.
- (3) Hu, Y. F.; Liu, Z. C.; Xu, C. M.; Zhang, X. M. *Chem. Soc. Rev.* **2011**, *40*, 3802–3823.
- (4) Hayashi, S.; Sata, S.; Hamaguchi, H. *IEEE Trans. Magn.* **2006**, *42*, 12–14.
- (5) Wang, H.; Yan, R.; Li, Z.; Zhang, X.; Zhang, S. *Catal. Commun.* **2010**, *11*, 763–767.
- (6) Iwata, K.; Okajima, H.; Saha, S.; Hamaguchi, H. *Acc. Chem. Res.* **2007**, *40*, 1174–1181.
- (7) Okuno, M.; Hamaguchi, H. *Appl. Phys. Lett.* **2006**, *89*, 132506–1–132506–2.
- (8) Hayashi, S.; Hamaguchi, H. *Chem. Lett.* **2004**, *33*, 1590–1591.
- (9) Kim, J.-Y.; Kim, J.-T.; Song, E.-A.; Min, Y.-K.; Hamaguchi, H. *Macromolecules* **2008**, *41*, 2886–2889.
- (10) Yoshida, Y.; Saito, G. *J. Mater. Chem.* **2006**, *16*, 1254–1262.
- (11) Bica, K.; Gaertner, P. *Org. Lett.* **2006**, *8*, 733–735.
- (12) Yin, D.; Li, C.; Tao, L.; Yu, N.; Hu, S.; Yin, D. *J. Mol. Catal. A: Chem.* **2006**, *245*, 260–265.
- (13) Shang, S.; Liang, L.; Yang, X.; Zheng, L. *J. Colloid Interface Sci.* **2009**, *333*, 415–418.
- (14) Lin, I. J. B.; Vasam, C. S. *J. Organomet. Chem.* **2005**, *690*, 3498–3512.
- (15) Song, E.-A.; Jung, W.-G.; Ihm, D.-W.; Kim, J.-Y. *Bull. Korean Chem. Soc.* **2009**, *30*, 1009–1011.
- (16) Li, J. G.; Hu, Y. F.; Ling, S.; Zhang, J. Z. *J. Chem. Eng. Data* **2011**, *56*, 3068–3072.
- (17) Cheng, J.; Yang, Y.; Tong, Y.; Lu, S.; Sun, J.; Zhu, K.; Liu, Y.; Siu, G. G.; Xu, Z. K. *J. Appl. Phys.* **2009**, *105*, 053519–1–053519–5.
- (18) Sitze, M. S.; Schreiter, E. R.; Patterson, E. V.; Freeman, R. G. *Inorg. Chem.* **2001**, *40*, 2298–2304.
- (19) Yang, J.-Z.; Xu, W.-G.; Zhang, Q.-G.; Jin, Y.; Zhang, Z.-H. *J. Chem. Thermodyn.* **2003**, *35*, 1855–1860.
- (20) Nguyen, M. D.; Nguyen, L. V.; Jeon, E. H.; Kim, J. H.; Cheong, M.; Kim, H. S.; Lee, J. S. *J. Catal.* **2008**, *258*, 5–13.
- (21) Papatheodorou, G. N.; Voyiatzis, G. A. *Chem. Phys. Lett.* **1999**, *303*, 151–156.
- (22) Hitchcock, P. B.; Seddon, K. R.; Welton, T. *J. Chem. Soc., Dalton Trans.* **1993**, 2639–2643.
- (23) Larsen, A. S.; Holbrey, J. D.; Tham, F. S.; Reed, C. A. *J. Am. Chem. Soc.* **2000**, *122*, 7264–7272.
- (24) Xie, Z.-L.; Taubert, A. *ChemPhysChem.* **2011**, *12*, 364–368.
- (25) Li, J. G.; Hu, Y. F.; Sun, S. F.; Ling, S.; Zhang, J. Z. *J. Chem. Thermodyn.* **2011**, submitted for publication.
- (26) Wang, Y. T.; Voth, G. A. *J. Phys. Chem. B* **2006**, *110*, 18601–18608 and ref 25 cited therein.
- (27) Neto, B. A. D.; Ebeling, G.; Gonçalves, R. S.; Gozzo, F. C.; Eberlin, M. N.; Dupont, J. *Synthesis* **2004**, 1155–1158.
- (28) Lecocq, V.; Graille, A. L.; Santini, C. C.; Baudouin, A.; Chauvin, Y.; Basset, J. M.; Arzel, L.; Bouchu, D.; Fenet, B. *New J. Chem.* **2005**, *29*, 700–706.
- (29) Shigeto, S.; Hamaguchi, H.-O. *Chem. Phys. Lett.* **2006**, *427*, 329–332.